Secondary optical element design for intracorporeal LED illumination system

Jui-Wen Pan,[1,2,3,*] Ying-Chieh Su,[1,4] and Yao-Shan Chen[5]

[1]*Institute of Photonic System, National Chiao Tung University, Tainan City 71150, Taiwan*

[2]*Department of Medical Research, Chi Mei Medical Center, Tainan City 71004, Taiwan*

[3]*Institute of Imaging and Biomedical Photonics System, National Chiao Tung University, Tainan City 71150, Taiwan*

[4]*Department of Thoracic Surgery, Chi Mei Medical Center, Tainan City 71004, Taiwan*

[5]*Biomedical Electronics Translational Research Center, National Chiao Tung University, Hsin-Chu City 30010, Taiwan*

**Corresponding author: juiwenpan@gmail.com*

Received October 2, 2013; revised November 12, 2013; accepted November 22, 2013;
posted November 25, 2013 (Doc. ID 198649); published January 6, 2014

In this Letter, we propose an intracorporeal illumination system for providing uniform and wide-field illumination during minimally invasive surgery. The illumination system is comprised of an Alexis wound retractor, a set of LEDs, and secondary optical elements (SOEs). The SOE was composed of a Fresnel lens and a total internal reflection lens, which was designed to improve the optical performance of the LED. The results of simulation demonstrate that the optical efficiency of each LED with an SOE could be increased from 33.6% to 82.9%. To avoid damage to human tissue by thermal effect, the number of LEDs with SOEs was optimized. The results indicate that our design to be applicable for practical surgery.

OCIS codes: (170.2945) Illumination design; (220.4298) Nonimaging optics; (220.2740) Geometric optical design.
http://dx.doi.org/10.1364/OL.39.000224

In minimally invasive surgery (MIS), the incision is smaller than a traditional surgical incision. However, the small size of the incision makes the illumination provided by the extracorporeal surgical task (EST) [1] light impractical. The EST light beam is obscured by the incision and the surgeon's head [2]. To solve the problems, the head-mounted surgical task (HMST) light has been developed. The illumination field is controlled by the rotation of the surgeon's head. Improved illumination is provided, but the surgeons using the light has to adapt to the sensation of dizziness caused by the focused light beam. The shelter effect from the incision still exists. Thus neither the EST light nor the HMST light are feasible for MIS. At the present time, surgeons use videoscopic systems to provide intracorporeal [3] light. The videoscopic system uses optical fiber to guide the light into the thoracic cavity. However, videoscopy has three major disadvantages: (1) the field of illumination is quite narrow; (2) the range of movement is restricted (the videoscope have to be removed from one incision before being placed into another; this means that extra incisions are required in MIS [4]); and (3) an operator is needed to ensure a correct illumination field. Clearly, a better intracorporeal surgical task light is desired to provide wide-field illumination in MIS.

In this Letter, we propose a design for an intracorporeal LED illumination system embedded within an Alexis wound retractor (AWR). With the application of the AWR [5] to keep open the surgical incision, the LEDs fixed on the interior ring of the AWR work like a ceiling lamp to illuminate the unilateral thoracic cavity. Considering the practical application of this design, the operation of LEDs will generate the heat in the thoracic cavity. This heat will not only reduce the optical efficiency of the LEDs [6], but also have an effect on human tissue [7]. A high-efficiency secondary optical element (SOE) is further included in the design of our proposed illumination system to keep the operating temperature of the illumination system at a level acceptable for human tissue [7]. Moreover, in order not to affect the surgeon in surgery, the illumination system must not be too thick, so the compact size of the SOE becomes important. The SOE is composed of a Fresnel lens and a total internal reflection (TIR) lens. The design can improve the optical efficiency of each LED and reduce the number of LEDs needed in the AWR. The designs of a Fresnel lens and the TIR lens for improving the optical efficiency of LEDs are clarified below. The relationship between the number of LED, the power consumption, and the temperature of the illumination system in the thoracic cavity were also investigated.

Figure 1 shows a diagram of the thoracic cavity with an incision opened by our designed illumination system. The model of the thoracic cavity with a length of 300 mm was built by using two kinds of software: AutoCAD and LightTools [8]. The geometrical thoracic cavity was captured from a random computer tomography (CT) image provided by ChiMei Hospital [9]. The illumination system consisted of a set of LEDs with SOEs embedded in the AWR. The diameter of the receiver was 150 mm. The distance between the illumination system and the receiver was 100 mm, a distance arrived at based on human statistical data [10]. Considering the width of the AWR's

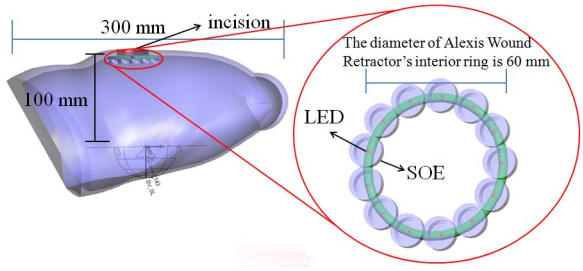

Fig. 1. Configuration of a thoracic cavity with our designed illumination system. The structure of the illumination system is an AWR embedded with LED and SOE.

interior ring and the condition of surgical operation as shown in Table 1, the LED used in the AWR was a Nichia NS2W157ART-H3 [11]. The luminous flux and size of the LED are 50 lm and 3 mm × 1.4 mm × 0.52 mm, respectively. The radiation pattern is Lambertian.

The number of LEDs for achieving the minimum illuminance in the thoracic cavity can be determined. The minimum illuminace is 40000 lux, as shown in Table 1, and the number of LEDs without SOEs, as obtained from numerical calculation, is 25. The total power consumption and the operating temperature of the illumination system are 13 W and 120°C, respectively. The optical efficiency of the LED without the SOE is 33.6%. Obviously, this would make the temperature of the designed illumination system too high to be acceptable to human tissue. To reduce the temperature effect, the number of LEDs is reduced by utilizing SOEs in the illumination system to concentrate the rays and thus increase the optical efficiency of each LED.

Owing to the characteristic of hemispherical radiation, the radiation angle of the LED is too large for the rays to be effectively collected by the receiver [13]. In our design, the SOE is composed of a Fresnel lens and TIR lens, both of which are responsible for collimating the rays at the given receiver [14]. Figure 2 shows the cross section of illumination system. The yellow and green areas indicate the Fresnel lens and TIR lens, respectively. The Fresnel lens can cover the radiation angle (ω_{FL}) range between 0° and 60°. The TIR lenses are designed for rays with radiation angles (ω_{TIR}) range from 61° to 90°. The SOE is also designed to be axis symmetrical with the prismatic facets facing toward the light source to avoid damage to the thoracic cavity. Based on these mechanisms, the design of SOE has two processes.

During the first process, the rays are collected by the Fresnel lens and guided into the receiver. The value of d, representing the distance between the LED and Fresnel lens, is a crucial parameter for determining the size of the Fresnel lens. In order to keep the volume of the SOE for our designed illumination system small, the value of d was set to be 2 mm. For the Fresnel lens design, the maximum radius (L) of the lens can be determined from Eq. (1), and the ray's exit angle β of the lens can be calculated with Eq. (2):

$$L = d \times \tan \omega_{FLM}, \tag{1}$$

$$\tan \beta = \frac{45 - L}{100 - d}. \tag{2}$$

As the maximum angle of the radiation ray collected by the Fresnel lens (ω_{FLM}) is 60°, the maximum radius L and the exit angle β are approximately equal to 3.46 mm and 23°, respectively. Subsequently, as shown in Fig. 3, the prism angle α defined as the angle between the incident ray and the normal of the Fresnel lens's facet [15] can be derived from Eq. (3):

$$\tan \alpha = \frac{R}{n_2 \sqrt{R^2 + d^2} - d}, \tag{3}$$

where n_2 and R are the refractive index of the Fresnel lens and the distance between the incident ray and the central axis of the Fresnel lens, respectively [16]. Considering the limitation of manufacturing the Fresnel lens and n_2 of 1.488, α has a minimum value of 30°. As a result, the minimum value of R, which can be regarded as the pitch size of each facet in the Fresnel lens is 0.65 mm. On the other hand, when R is equal to L, the maximum prism angle α_{max} is 41.24° for the outermost ring of the Fresnel lens.

Considering the second process, the rays with radiation angle (ω_{TIR}) from 61° to 90° are collimated by the TIR lens, based on the Snell's law and the principles of TIR shown in Fig. 3. According to Snell's law, the relationship between ω_{TIR} and the refractive angles φ at the first refractive facet can be described by

Table 1. Conditions of Illumination for Surgical Operation [12]

Item	Value
Color rendering index (CRI)	>85
Color temperature	3000–6700 K
Illuminance	≥40 klux

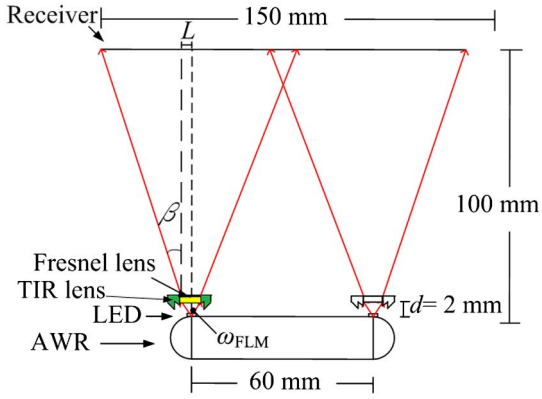

Fig. 2. Cross section of the illumination system. Red lines indicate the propagation of refraction rays.

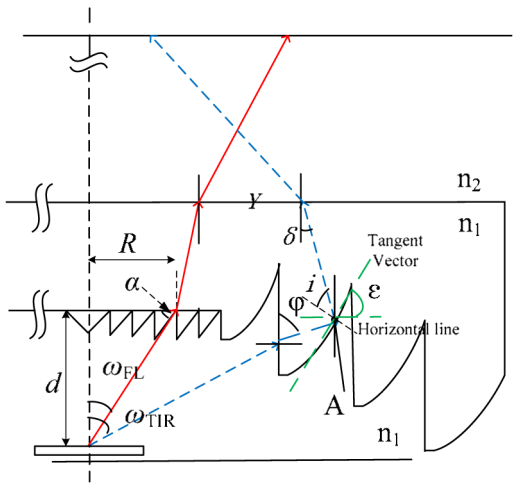

Fig. 3. Structure and geometrical analysis of SOE. The red and blue lines indicate the refractive and reflective lights, respectively. The green line means the tangent vector on the reflective surface.

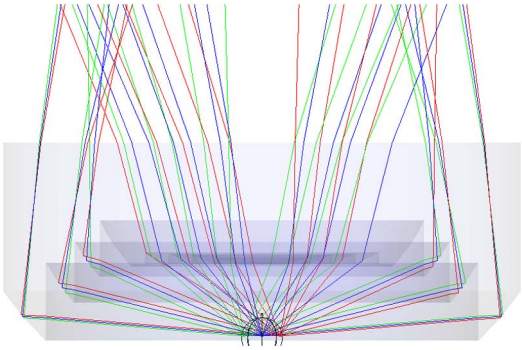

Fig. 4. Ray fan for the LED light source with SOE.

$$n_1 \sin(90° - \omega_{\mathrm{TIR}}) = n_2 \sin(90° - \varphi). \quad (4)$$

The rays are reflected by the TIR surface at point A. i is the TIR angle, and the critical angle is 42.22°. The angle ε represents the direction of the tangent vector at point A with respect to the horizontal lines. Therefore we can obtain the following relationship shown in Eq. (5) and Eq. (6) [17,18]:

$$2i + \delta + \varphi = 180°, \quad (5)$$

$$\varepsilon + \varphi + i = 180°, \quad (6)$$

where δ and γ are the incident angle and the output angle of the ray on the last surface, respectively. According to Snell's law, the relation between δ and γ is formulated as in Eq. (7):

$$n_2 \sin \delta = n_1 \sin \gamma, \quad (7)$$

where n_1 and n_2 are the refractive indices of air and polymethyl methacrylate (PMMA), respectively. The value of n_1 is 1, and the value of n_2 is 1.488. From Eqs. (4), (5), (6), and (7), the value of the ε on the curve of the reflective surface can be obtained. Thus the curve of TIR lens can composed of the tangent vector slope [19]. In order to reduce the rays without hitting the curve, each low point of one curve and the high point of the next curve must be on the same line.

After discussing the mechanisms involved in the design of the Fresnel lens and the TIR lens for collimating the rays at the receiver, the propagation of light emitted from the LED and the optical performance were simulated by LightTools. In this simulation, the material of the SOE is PMMA [20]. The optimized thickness and diameter of the SOE were 5.4 and 14.15 mm, respectively. Figure 4 shows the ray fan for the designed SOE with an LED light source. Clearly, most of rays are collected by the receiver. The optical efficiency of the LED with SOE increased from 33.6% to 82.9%. In further discussion of the effect of the SOE on the intensity distribution of the LED, we found that the radiation angle of the LED could be reduced from 120° to 46° simply by incorporating the SOE on the LED, as shown in Fig. 5. In addition to the feature of collimating the rays, our proposed SOE design is more compact in size than the currently available SOEs [21] and will not cause injury to the thoracic cavity, making it more feasible for MIS application.

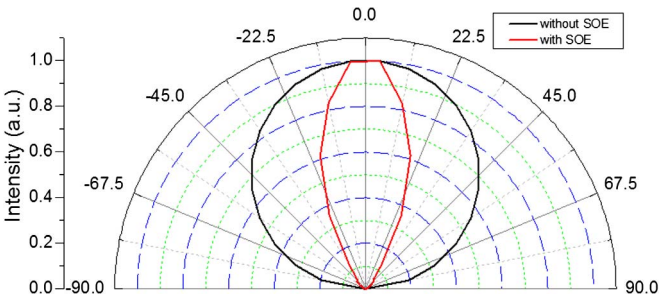

Fig. 5. Relative intensity distribution of a LED light source without SOE and with SOE.

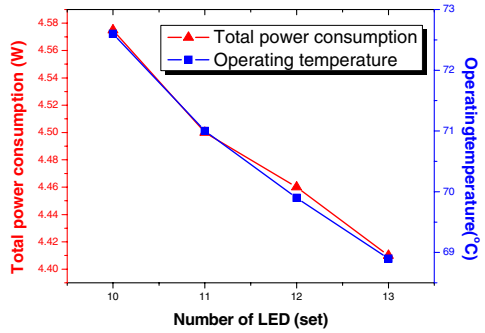

Fig. 6. Relation among the number of LEDs, total power consumption, and temperature after the illumination system with SOE.

Owing to increases in the optical efficiency per LED as a consequence of incorporation of SOEs, the number of LEDs fixed on the AWR can be reduced to 10. Considering the size of the SOEs and the AWR, the maximum

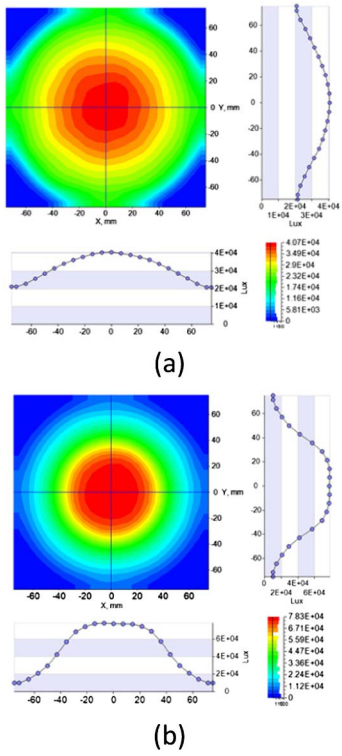

Fig. 7. Illuminance distribution of the illumination system: (a) without SOE and (b) with SOE.

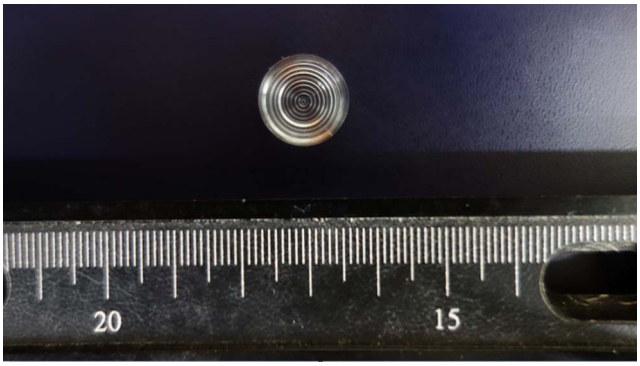

Fig. 8. Photograph of the SOE sample.

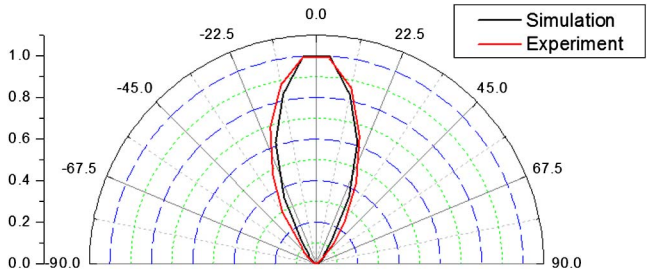

Fig. 9. Relative intensity distribution of a LED light source at simulation and experiment.

number of LEDs needed is 13. In order to find the appropriate value for improving the total power and temperature, we further optimized the number of LED. Figure 6 presents the changes of temperature and total power consumption of the illumination system with SOEs as a function of the number of LEDs. The total luminous flux for the illumination system obtained with a different number of LEDs is controlled by adjusting the current of all LEDs. This result suggests that the temperature and power consumption of the system are decreased with increasing the number of LEDs. As a result, the total power consumption and operating temperature of the AWR embedded with 13 sets of LED and SOE are 4.41 W and 68°C, respectively. With further discussion on the illuminance distribution, as shown in Fig. 7, it can be found that the SOE illumination system is more concentrated than of the illumination system without SOEs, implying effective collection of the rays at the receiver. This result also indicates an effective increased of the ray's intensity in the illumination system with SOE.

The finished SOE is shown in Fig. 8. In order to verify the optical performance of the SOE with LED design, we measured the intensity distribution of the LEDs. As can be seen in Fig. 9, in the experiment the radiation angle is 49.6°. The resultant error is 7%.

In conclusion, we present a design of an AWR embedded with LEDs and SOEs to form an illumination system to improve intracorporeal illumination during surgery. An SOE, consisting of a Fresnel lens and a TIR lens, is used with each LED to collect the rays effectively at the receiver. By optimizing the geometrical structure of the Fresnel lens and the TIR lens, the optical efficiency of each LED with SOE can be improved to 82.9%. As a result, the SOE illumination system enables the reduction of total power consumption from 13 to 4 W and a drop in operating temperature from 120°C to 68°C. Although 40° C is the acceptable temperature for human thoracic cavity, a water pipe circulation system is included in our illumination system design to further reduce the operating temperature as well as the power consumption. We believe that our proposed illumination system can make the surgery easier.

This study was supported in part by the National Science Council, project numbers NSC101-2220-E-009-006, NSC101-2622-E-009-010-CC3 and in part by the Chi Mei Medical Center, projector number 102C043, and in part by the "Aim for the Top University Plan" of the National Chiao Tung University and the Ministry of Education, Taiwan.

References

1. U. R. Shettigar, J. Membr. Sci. **44**, 89 (1989).
2. Berchtold, http://www.berchtold.biz/de/node/1950.
3. J. W. Collins and N. P. Wiklund, Eur. Urol. **63**, 644 (2013).
4. F. S. Tsai, D. Johnson, S. H. Cho, W. Qiao, A. Arianpour, and Y. H. Lo, in *Proceedings of IEEE Conference on Engineering in Medicine, and Biology Society* (IEEE, 2009), pp. 4081–4084.
5. Applied Medical, http://www.apliedmedical.com/Products/Alexis.aspx.
6. B. Siegal, in *Proceedings of IEEE International Electronics Manufacturing Technology Conference* (IEEE, 2007), pp. 62–66.
7. A. Prabath, *The Building Environment: Active and Passive Control Systems* (Wiley, 2006), Chap. 1.
8. Lighttools, CYBERNET SYSTEMS TAIWAN Co. Ltd., http://www.opticalres.com/.
9. Chi Mei Hospital, http://www.chimei.org.tw/.
10. G. Simon and G. Gamsu, Am. J. Roentgenol. **128**, 239 (1977).
11. Nichia NS2W157ART-H3, http://www.nichia.co.jp/specification/en/product/led/NS2W157AR-H3-E.pdf.
12. IEC Standard Danmark, http://www.dmts.dk/kongres/09/IEC%20STANDARD%20DENMARK.pdf.
13. J. W. Pan, S. H. Tu, C. M. Wang, and J. Y. Chang, Appl. Opt. **47**, 3406–3414 (2008).
14. J. Y. Joo, C. S. Kang, S. S. Park, and S. K. Lee, Opt. Express **17**, 23449 (2009).
15. R. Leutz and A. Suzuki, *Nonimaging Fresnel Lenses* (Springer, 2001), Chap. 4.
16. J. W. Pan, J. Y. Huang, C. M. Wang, H. F. Hong, and Y. P. Liang, Opt. Commun. **284**, 4283 (2011).
17. Y. Guiying, D. Shushu, J. Ji, and G. Tiantai, Proc. SPIE **8321**, 832110 (2011).
18. J. J. Chen and C. T. Lin, Proc. SPIE **49**, 093001 (2010).
19. J. J. Chen, T. Y. Wang, K. L. Huang, T. S. Liu, M. D. Tsai, and C. T. Lin, Opt. Express **20**, 10984 (2012).
20. C. Dorronsoro, D. Cano, J. Merayo-Lloves, and S. Marcos, Opt. Express **14**, 6142 (2006).
21. LedLink, http://www.ledlink-optics.com/ProductsHomeLED.aspx.